Elemental Compositions of Comet 81P/Wild 2 Samples Collected by Stardust

George J. Flynn, *et al.*

Science **314**, 1731 (2006);
DOI: 10.1126/science.1136141

References and Notes

1. M. J. Mumma, P. R. Weissman, S. A. Stern, In *Protostars and Planets III*, E. H. Levy, J. I. Lunine, M. S. Matthews, Eds. (Univ. of Arizona Press, Tucson, AZ, 1993), pp. 1172–1252.
2. J. D. Bregman *et al.*, *Astron. Astrophys.* **187**, 616 (1987).
3. J. D. Bregman *et al.*, *Astron. Astrophys.* **334**, 1044 (1988).
4. H. Campins, E. V. Ryan, *Astrophys. J.* **341**, 1059 (1989).
5. F. J. Molster, L. B. F. M. Waters, in *Astromineralogy, Lecture Notes in Physics*, T. K. Henning, Ed. (Springer, Berlin, 2003), pp. 121–170.
6. D. H. Wooden *et al.*, *Astrophys. J.* **517**, 1034 (1999).
7. D. E. Harker *et al.*, *Astrophys. J.* **580**, 579 (2002).
8. C. M. Lisse *et al.*, *Science* **313**, 635 (2006).
9. F. J. M. Rietmeijer, *Rev. Mineral.* **36**, 95 (1998).
10. J. P. Bradley, in *Treatise on Geochemistry,* vol. 1, H. D. Holland, K. K. Turekian, Eds. (Elsevier, Oxford, 2004), pp. 1121–1140.
11. D. E. Brownlee *et al.*, *Science* **314**, 1711 (2006).
12. S. A. Sandford *et al.*, *Science* **314**, 1720 (2006).
13. S. A. Sandford *et al.*, *Astrophys. J.* **371**, 607 (1991).
14. L. P. Keller *et al.*, *Geochim. Cosmochim. Acta* **68**, 2577 (2004).
15. K. D. McKeegan *et al.*, *Science* **314**, 1724 (2006).
16. G. J. Flynn, L. P. Keller, M. Feser, S. Wirick, C. Jacobsen, *Geochim. Cosmochim. Acta* **67**, 4791 (2003).
17. G. Matrajt *et al.*, *Astron. Astrophys.* **433**, 979 (2005).
18. P. Ehrenfreund, F. Robert, L. D'Hendencourt, F. Behar, *Astron. Astrophys.* **252**, 712 (1991).
19. A. Gardinier *et al.*, *Earth Planet. Sci. Lett.* **184**, 9 (2000).
20. Y. J. Pendleton, L. J. Allamandolla, *Astrophys. J. Suppl. Ser.* **138**, 75 (2002).
21. Y. J. Pendleton *et al.*, *Astrophys. J.* **437**, 683 (1994).
22. D. C. B. Whittet *et al.*, *Astrophys. J.* **490**, 729 (1997).
23. J. E. Chiar *et al.*, *Astrophys. J.* **537**, 749 (2000).
24. E. Dartois *et al.*, *Astron. Astrophys.* **423**, 549 (2004).
25. M. A. DiSanti *et al.*, *Icarus* **116**, 1 (1995).
26. M. E. Zolensky *et al.*, *Science* **314**, 1735 (2006).
27. J. Dorschner, T. Henning, *Astron. Astrophys. Rev.* **6**, 271 (1995).
28. F. Kemper, W. J. Vriend, A. G. G. M. Tielens, *Astrophys. J.* **609**, 826 (2004).
29. F. Kemper, W. J. Vriend, A. G. G. M. Tielens, *Astrophys. J.* **633**, 534 (2005).
30. J. P. Bradley *et al.*, *Science* **285**, 1716 (1999).
31. G. J. Flynn, L. P. Keller, *Workshop on Cometary Dust in Astrophysics*, LPI Contribution No. 1182, #6053 (2003).
32. J. Crovisier *et al.*, *Science* **275**, 1904 (1997).
33. L. P. Keller, S. Messenger, *Lunar Planet Sci.* **35**, 1985 (2004).

34. We thank L. Carr and R. Smith for providing key support for the far-IR measurements at the National Synchrotron Light Source, Brookhaven National Laboratory; M. Martin and Z. Hao at the Advanced Light Source, Lawrence Berkeley National Laboratory; and the personnel of Assing S.p.A. for their availability and technical assistance. Supported by grants from the NASA Cosmochemistry and Origins programs (L.P.K.) Some of this work was performed in part under the auspices of the U.S. Department of Energy by the Lawrence Livermore National Laboratory under contract W-7405-ENG-48. The Advanced Light Source is supported by the Office of Basic Energy Sciences, Materials Sciences Division, of the U.S. Department of Energy under contract DE-AC03-76F00098 at Lawrence Berkeley National Laboratory. The work was also supported by the Università di Napoli "Parthenope," INAF, and MIUR.

Supporting Online Material

www.sciencemag.org/cgi/content/full/314/5806/1728/DC1
SOM Text

2 October 2006; accepted 15 November 2006
10.1126/science.1135796

REPORT

Elemental Compositions of Comet 81P/Wild 2 Samples Collected by Stardust

George J. Flynn,[1]* Pierre Bleuet,[2] Janet Borg,[3] John P. Bradley,[4] Frank E. Brenker,[5] Sean Brennan,[6] John Bridges,[7] Don E. Brownlee,[8] Emma S. Bullock,[9] Manfred Burghammer,[2] Benton C. Clark,[10] Zu Rong Dai,[4] Charles P. Daghlian,[11] Zahia Djouadi,[3] Sirine Fakra,[12] Tristan Ferroir,[13] Christine Floss,[14] Ian A. Franchi,[7] Zack Gainsforth,[15] Jean-Paul Gallien,[16] Philippe Gillet,[13] Patrick G. Grant,[4] Giles A. Graham,[4] Simon F. Green,[7] Faustine Grossemy,[3] Philipp R. Heck,[17] Gregory F. Herzog,[18] Peter Hoppe,[17] Friedrich Hörz,[19] Joachim Huth,[17] Konstantin Ignatyev,[6] Hope A. Ishii,[4] Koen Janssens,[20] David Joswiak,[8] Anton T. Kearsley,[21] Hicham Khodja,[16] Antonio Lanzirotti,[22] Jan Leitner,[23] Laurence Lemelle,[13] Hugues Leroux,[24] Katharina Luening,[6] Glenn J. MacPherson,[9] Kuljeet K. Marhas,[14] Matthew A. Marcus,[12] Graciela Matrajt,[8] Tomoki Nakamura,[25] Keiko Nakamura-Messenger,[26] Tsukasa Nakano,[27] Matthew Newville,[22] Dimitri A. Papanastassiou,[28] Piero Pianetta,[6] William Rao,[29] Christian Riekel,[2] Frans J. M. Rietmeijer,[30] Detlef Rost,[9] Craig S. Schwandt,[26] Thomas H. See,[26] Julie Sheffield-Parker,[31] Alexandre Simionovici,[13] Ilona Sitnitsky,[1] Christopher J. Snead,[15] Frank J. Stadermann,[14] Thomas Stephan,[23] Rhonda M. Stroud,[32] Jean Susini,[2] Yoshio Suzuki,[33] Stephen R. Sutton,[22] Susan Taylor,[34] Nick Teslich,[4] D. Troadec,[24] Peter Tsou,[28] Akira Tsuchiyama,[35] Kentaro Uesugi,[33] Bart Vekemans,[20] Edward P. Vicenzi,[9] Laszlo Vincze,[36] Andrew J. Westphal,[15] Penelope Wozniakiewicz,[21] Ernst Zinner,[14] Michael E. Zolensky[19]

We measured the elemental compositions of material from 23 particles in aerogel and from residue in seven craters in aluminum foil that was collected during passage of the Stardust spacecraft through the coma of comet 81P/Wild 2. These particles are chemically heterogeneous at the largest size scale analyzed (~180 ng). The mean elemental composition of this Wild 2 material is consistent with the CI meteorite composition, which is thought to represent the bulk composition of the solar system, for the elements Mg, Si, Mn, Fe, and Ni to 35%, and for Ca and Ti to 60%. The elements Cu, Zn, and Ga appear enriched in this Wild 2 material, which suggests that the CI meteorites may not represent the solar system composition for these moderately volatile minor elements.

NASA's Stardust spacecraft collected dust particles from comet 81P/Wild 2, at an encounter speed of ~6.1 km/s, in silica aerogel capture cells and in impact craters (*1*). Analytical results from the aerogel and foils were combined to provide a more comprehensive elemental analysis of the Wild 2 particles.

The impacts in aerogel produced elongated cavities called tracks. Wedges of aerogel, called keystones (*2*), containing an entire track were extracted. The volume containing each track was analyzed by means of synchrotron-based x-ray microprobes (SXRMs), providing abundances for elements having an atomic number $Z \geq 16$ (S). One track was subsequently split open, exposing the wall for time-of-flight–secondary ion mass spectrometry (TOF-SIMS) analysis, detecting lower-Z elements, particularly Mg and Al. Because Si and O are the major elements in silica aerogel, neither element could be determined in the comet material in tracks. The residues in craters were analyzed by scanning electron microscopy using energy-dispersive x-ray (SEM-EDX) analyses and TOF-SIMS, providing other element abundances, including Mg and Si.

The SXRMs produce intense, focused beams of x-rays that completely penetrate a keystone, exciting fluorescence (*3*). Elemental analysis was performed on keystones containing 23 tracks, which were selected to sample the diversity on the collector, by seven research groups with the use of six different SXRMs (*4*). These tracks range in length from ~250 μm to almost 10,000 μm and vary in shape from conical to bulbous. The Fe content of the tracks varies from ~180 fg to 6.4 ng (table S3), comparable to the Fe in chondritic particles ranging from ~1 to ~30 μm in size. All 23 tracks were approximately normal to the aerogel surface, which was the arrival direction for particles collected from Wild 2 (*1*), whereas interplanetary particles, also collected, arrived over a wide range of orientations. Comets are thought to preserve dust from the early solar system, so we compared the Wild 2 dust to the elemental composition of the CI meteorites (CI) (*5*) because CI is thought to represent the nonvolatile composition of the solar system (*6*).

A map of the K-alpha fluorescence intensity for Fe from a conical track, track 19, shows that the incident particle deposited Fe along much of the entry path (Fig. 1), with only 3% of the total Fe contained in the terminal particle. The fraction of the total Fe detected in the terminal particle varies from track to track, ranging from almost 60% in one terminal particle to zero in two tracks having no detectable terminal particle. In most of the 23 tracks, most of the incident Fe mass is unevenly distributed along the track, indicating that the

particles are relatively weak. Their behavior during aerogel capture is most like that observed when grains from mechanically weak meteorites, such as Orgueil, are shot at high velocities into aerogel.

The spatial distributions of other elements in each track vary widely (*4*). Nickel is deposited along the entire length of track 19 (Fig. 1). The Ni/Fe ratio summed over the whole track is 0.041, which is within 50% of the CI ratio (0.058) (*5*). However, Ni/Fe is much lower (0.0062) in the terminal particle, demonstrating elemental heterogeneity. Zinc is concentrated along one edge of the track, with almost none detectable in the terminal particle, but ~80% of the total Cr is in the terminal particle.

The terminal particle and the 19 most intense element hot spots along track 19 were analyzed individually, with the use of much longer acquisition times than at each pixel in the maps. Most element/Fe ratios vary by more than two orders of magnitude from spot to spot along this track (Fig. 1). A "whole-track" composition for track 19 (Fig. 1) was determined by adding the element abundances from these 20 analyses. The S/Fe, Cr/Fe, Mn/Fe, and Ni/Fe ratios are similar to the CI values, but the moderately volatile elements Cu, Zn, Ga, and Se are higher than CI, and Ca and Ge are lower.

The whole-track composition for track 19 differs significantly from the composition of the terminal particle (Fig. 1), with the moderately volatile elements being much lower in the terminal particle. Many terminal particles have elemental compositions that are consistent with their being dominated by a single mineral, generally olivine, pyroxene, or sulfide, a result confirmed by mineralogical examination of some extracted particles (*7*). Thus, terminal particle analysis provides limited information on the bulk elemental composition of Wild 2.

No single mineral found in terrestrial or extraterrestrial material has a CI composition. So, a CI composition indicates that the particle is a mixture of compositionally diverse grains. The high variability of the 20 spot analyses along track 19 (Fig. 1) further indicates the particle was an aggregate of diverse grains. However, not all tracks demonstrate near-CI abundances (Fig. 2).

We determined the mean composition of the comet material by summing the measured abundance of each element over all 23 tracks (Table 1 and Fig. 3). The aerogel contains trace quantities of virtually all stable elements (*1*), and several elements are found in hot spots (fig. S1), complicating background subtraction (*4*).

The widespread distribution of compositionally diverse comet material and contamination along most tracks required the development of analytical strategies that provided the most comprehensive set of element analyses. Tracks were analyzed in different laboratories by means of two complementary methods. For some keystones, an entire fluorescence spectrum was collected, with the use of a long integration time, at each point in a raster scan over the whole track. Other keystones were analyzed by identifying "hot spots" in a quick scan and then dwelling for much longer times on these hot spots. The first technique provides more reliable data for elements in high abundance, whereas the second is more sensitive for trace elements. The mean, blank-corrected compositions obtained through the two techniques are very similar (fig. S6), indicating that any systematic differences between the two techniques are smaller than the statistical errors in each data set (*4*).

Iron was detected in all 23 tracks; Ni in 22; S in 21; Ca, Cr, Mn, and Cu in 20; Zn in 17; Ga in 14; and Ti and Se in 9 (table S3). When an element was not detected, its concentration was recorded as zero in calculating the central value and lower limit on the mean. This technique underestimates the central value of the mean for low-abundance elements. It also underestimates the lower limit, leading to an overly conservative confidence interval (*4*). The

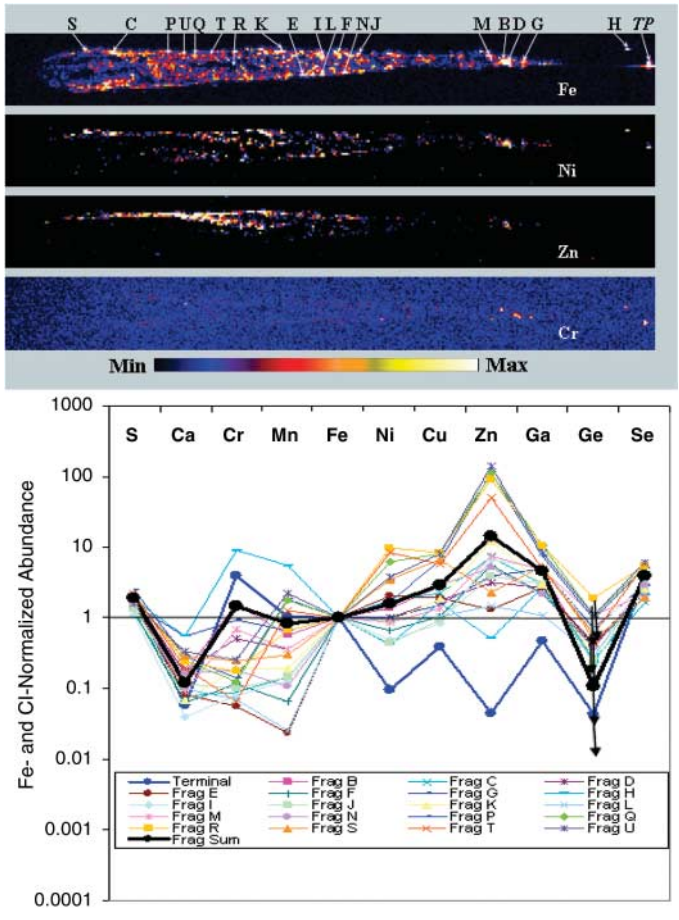

Fig. 1. X-ray fluorescence analysis results obtained on track 19, an 860-μm-long track. Maps of the Fe, Ni, Zn, and Cr fluorescence intensities were obtained with a step size of 3 μm per pixel and a dwell time of 0.5 s per pixel. The CI- and Fe-normalized element abundances for the terminal particle (TP) and the 19 most-intense element hot spots (letters B, C to N, P to U), whose positions are indicated on the Fe map, are plotted along with the whole-track average composition, determined by adding the element abundances from 19 spot analyses along the track and the analysis of the terminal particle. The horizontal line at 1 is the CI meteorite composition, which is thought to represent the mean solar system composition. Arrows indicate that all Ge analyses for these particles were upper limits.

[1]Department of Physics, State University of New York at Plattsburgh, 101 Broad Street, Plattsburgh, NY 12901, USA. [2]European Synchrotron Radiation Facility, Grenoble, France. [3]Institut d'Astrophysique Spatiale, Orsay, France. [4]Institute of Geophysics and Planetary Physics, Lawrence Livermore National Laboratory, Livermore, CA 94550, USA. [5]Institut für Mineralogy, Johann Wolfgang Goethe-Universität, Frankfurt, Germany. [6]Stanford Linear Accelerator Center, Menlo Park, CA 94025, USA. [7]The Open University, Milton Keynes, MK7 6AA, UK. [8]Department of Astronomy, University of Washington, Seattle, WA 98195, USA. [9]Department of Mineral Sciences, Smithsonian Institution, Washington, DC 20560, USA. [10]Lockheed Martin, Post Office Box 179, Denver, CO 80201, USA. [11]Dartmouth College, Hanover, NH 03755, USA. [12]Advanced Light Source, Lawrence Berkeley National Laboratory, Berkeley, CA 94720, USA. [13]École Normale Supérieure de Lyon, Lyon, France. [14]Washington University, St. Louis, MO 63130, USA. [15]Space Sciences Laboratory, University of California, Berkeley, CA 94720, USA. [16]Laboratory Pierre Süe, CEA/CNRS, Saclay, France. [17]Max Planck Institute for Chemistry, Mainz, Germany. [18]Department of Chemistry and Chemical Biology, Rutgers University, Piscataway, NJ 08854, USA. [19]NASA Johnson Space Center, Houston, TX 77058, USA. [20]Department of Chemistry, Universiteit Antwerpen, Antwerp, Belgium. [21]Department of Mineralogy, The Natural History Museum, London, SW7 5BD, UK. [22]The University of Chicago, Chicago, IL 60637, USA. [23]Institut für Planetologie, Universität Münster, 48149 Münster, Germany. [24]University Lille, Lille, France. [25]Kyushu University, Fukuoka, Japan. [26]Engineering and Science Contract Group/Jacobs Sverdrup, NASA Johnson Space Center, Houston, TX 77058, USA. [27]Geological Survey of Japan, National Institute of Advanced Industrial Science and Technology, Tsukuba, Japan. [28]Jet Propulsion Laboratory, California Institute of Technology, Pasadena, CA 91109, USA. [29]University of Georgia, Athens, GA 30602, USA. [30]Department of Earth and Planetary Sciences, University of New Mexico, Albuquerque, NM 87131, USA. [31]XRT Limited, Port Melbourne, Australia. [32]U.S. Naval Research Laboratory, Washington, DC 20375, USA. [33]Japan Synchrotron Radiation Research Institute/SPring-8, Hyougo, Japan. [34]Engineering Research and Development Center/Cold Regions Research and Engineering Laboratory, Hanover, NH 03755, USA. [35]Osaka University, Toyonaka, Japan. [36]Ghent University, Ghent, Belgium.

*To whom correspondence should be addressed. E-mail: george.flynn@plattsburgh.edu

CI-normalized whole-track element/Fe ratios (Fig. 2) exhibit variations of more than two orders of magnitude from track to track. Thus, a reliable mean composition can only be determined by averaging many tracks.

There are four major sources of error in the mean composition of the particles that produced the tracks: (i) the precision and accuracy of the analyses, (ii) absorption corrections in the capture medium and the particles themselves, (iii) the extent to which the material analyzed is representative of all the material in the initial particle, and (iv) uncertainty resulting from averaging only a small number of samples having extremely diverse compositions.

The SXRM abundances are accurate to ±20% for the elements having $Z \geq 24$ (Cr), and absorption corrections are small for elements having $Z \geq 20$ (Ca) (*4*). In no case can we be certain that we analyzed all the material from any incident particle. The extent to which vaporized material can be lost through the entry hole of a track has yet to be investigated. Vaporized material may also penetrate many track diameters through the aerogel, as observed for some organic matter in Wild 2 tracks (*8*). In addition, the spot analysis used for nine of the tracks only analyzed material in these hot spots. Nonetheless, the largest uncertainty in the mean composition is likely to result from the high degree of compositional heterogeneity among the particles (*4*). This uncertainty was estimated by means of a Monte Carlo method that assumes the particle sizes and compositions of the 23 measured tracks are characteristic of the entire dust population hitting the collector and determines 1 SD (1σ) and 2σ confidence limits from the distributions of elements in ensembles randomly picked from the observed data set (*4*).

Summing all 23 tracks, the Fe-normalized mean element abundances (Table 1) for Ca, Ti, Cr, Mn, Ni, Ge, and Se are consistent with CI values at the 2σ confidence level (Fig. 3). Because Ge and Se were detected in only a few particles, their central values and lower limits may be underestimated (*4*). Sulfur is depleted, and Cu, Zn, and Ga are enriched (Table 1).

One keystone, track 21, was dissected laterally to expose the track wall, and two slices were analyzed by TOF-SIMS (table S1). These analyses indicate that Mg/Fe, Al/Fe, Cr/Fe, and Mn/Fe are within 50% of CI (*4*).

Analysis of impact residue, which is abundant in all large craters in the Al foils examined, provides element-to-Si ratios. These Al foils contain indigenous Fe inclusions, occasional Si-rich inclusions, and a wide range of trace elements, but unambiguous impact residue was easily located in craters by both SEM-EDX and TOF-SIMS.

To assess element loss during crater production, we fired a variety of projectiles into Al1100 foil, the type flown on Stardust, with impact velocities of ~6 km/sec. In craters >50 μm in diameter, the loss of S, Na, Mg, Si, and Fe was small (*9*) (fig. S9), so analysis of residue in large craters is expected to provide a good sample of the composition of Wild 2 dust. Seven craters, each having a diameter >50 μm, were characterized by means of SEM-EDX (table S2).

The mass of each impacting particle, estimated through the crater-size calibration of Kearsley *et al.* (*10*) scaled by particle density appropriate for the mineralogy inferred from its chemical composition (*4*), ranges from 3 to 178 ng, with six having impactor masses of 17 ng or less (table S2). Only Mg, Si, and Fe were detected in all seven craters, Cr in four, Na in three, and P, K, Mn, and Ni in only two. Confidence limits on the mean abundances were modeled with the use of the same Monte Carlo technique used for the track data.

The CI- and Si-normalized mean composition for elements detected in four or more craters (Table 2) is within 50% of CI for Mg, Ca, and Fe. Depletions in S, Ca, Cr, and Fe, relative to that of Si, are significant at the 2σ confidence level (Fig. 4). The S depletion is consistent with the results

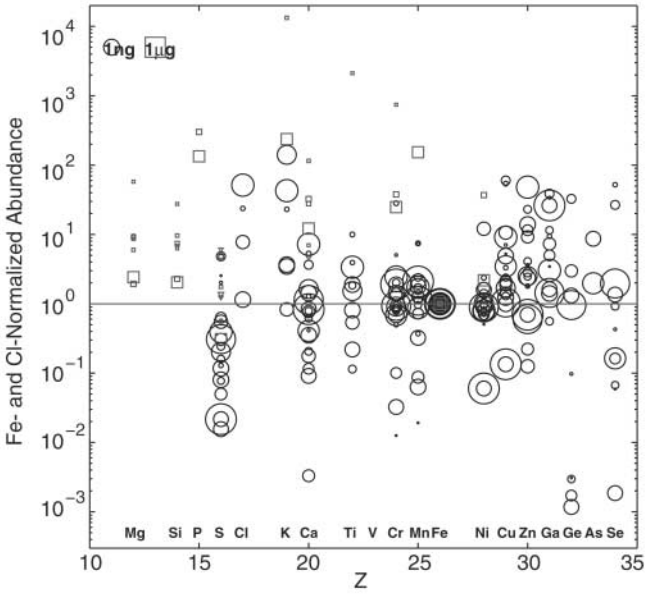

Fig. 2. CI- and Fe-normalized abundance for each element in each of the 23 whole tracks (circles) and in each of the seven crater residues (squares). The area of each data point is proportional to the cross section of an equant particle of equivalent mass. Because much larger masses were analyzed in the craters, there is a difference in the scale size of the two symbols by three orders of magnitude. There is a high degree of variability from track to track, with most elements varying by two orders of magnitude or more.

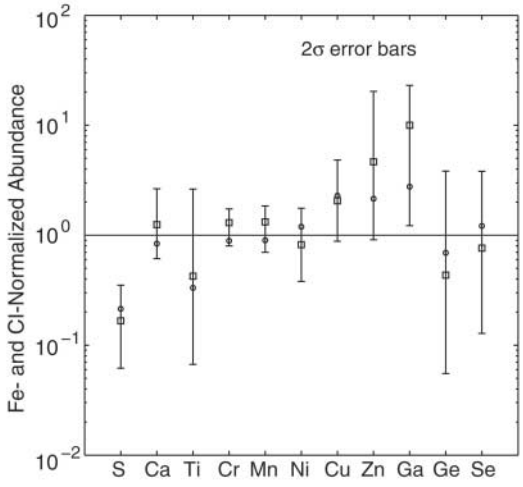

Fig. 3. CI- and Fe-normalized mean composition determined by summing the 23 whole-track analyses (squares) and by summing the same data set except for the particle having the highest Fe content (circles). One track contributed ~30% of the total Fe, but its inclusion does not distort the mean composition, because the mean excluding this track does not differ significantly from the 23-track mean. The vertical bars show the 2σ variation in the mean of a Monte Carlo simulation designed to assess the effect of this elemental diversity on the mean composition (*4*).

Table 1. Comparison of the mean composition of the material in the 23 tracks with the CI meteorite composition, with a CI- and Fe-normalized value of 1 indicating exact agreement between the total amount of that element detected in all the tracks and that expected if the particles had a CI composition. 1σ confidence limits are given.

Element	CI- and Fe-normalized abundance	1σ confidence limit (upper, lower)
S	0.17	+0.12, −0.06
Ca	1.25	+0.47, −0.43
Ti	0.42	+1.74, −0.23
Cr	1.30	+0.24, −0.31
Mn	1.32	+0.32, −0.37
Ni	0.82	+0.37, −0.24
Cu	2.06	+1.14, −0.69
Zn	4.60	+6.30, −3.10
Ga	10.00	+8.90, −7.50
Ge	0.43	+1.46, −0.22
Se	0.76	+1.51, −0.42

from the tracks. Higher Ca and Cr were found in the tracks (Fig. 3), but the 2σ confidence limits overlap for both elements in the track and crater analyses. Elements with less than four measurements were not reported in Table 2 because confidence limits were difficult to determine with so few detections, but the mean values obtained were Mn = 1.2 × CI, K = 0.7 × CI, Na = 1.6 × CI, and Ni = 0.2 × CI.

The residues in five of these craters were analyzed by TOF-SIMS (table S4). Calibration shots of mineral standards into Al foil demonstrate good agreement for most elements between TOF-SIMS analyses of impact residue and SEM-EDX analyses of unshot projectile material, but Na and K are sometimes higher in the TOF-SIMS analyses (fig. S11). The Si-normalized mean abundances (Fig. 4) are consistent with CI for Mg, Ca, and Ni, but there are small depletions for Cr and Fe, which are consistent with the SEM-EDX results. Lithium, Na, and K are enriched. Most of the Na and K detected by TOF-SIMS was found in a single crater (table S4), but SEM-EDX analysis of Na and K in residue in the same crater gives results that are an order of magnitude lower (table S2). This difference may result from SEM-EDX measuring micrometers into the residue, predominately at the crater bottom, whereas TOF-SIMS only measures material sputtered from the surface, mainly from the crater lip (*4*). The TOF-SIMS analyses in two different orientations show significantly different Na and K abundances (table S4), which suggests a very heterogeneous distribution, making it difficult to determine a mean abundance.

An SEM survey of the Al foils identified many smaller impact craters, generally <2 μm in diameter, corresponding to projectiles from ~20 to ~400 nm in diameter (*10*). SEM-EDX analysis of residue in several hundred small craters identified compositional groups that are consistent with impacting particles composed of silicates, sulfides, and mixtures of silicate and sulfide (*11*). However, the mass-frequency distribution of impacting particles (*11*) indicates that most of the mass collected at Wild 2 is in larger projectiles, so the total mass of material in the small craters is inadequate to substantially alter the mean element abundances measured on tracks and larger craters.

Table 2. Comparison of the mean composition of the material in the seven crater residues with the CI meteorite composition, with a CI- and Fe-normalized value of 1 indicating exact agreement. 1σ confidence limits are given.

Element	CI- and Si-normalized abundance	1σ confidence limit (upper, lower)
Mg	1.13	+0.22, −0.05
S	0.13	+0.40, −0.06
Ca	0.51	+0.12, −0.05
Cr	0.31	+0.31, −0.04
Fe	0.75	+0.05, −0.40

Sulfur is depleted in both the tracks and craters. The statistical significance of this depletion is high. Sulfur is highly variable in chondritic meteorites. Of the major elements, S shows the most extreme variation, being lower by a factor of five in ordinary chondrites than in CI meteorites. However, for the tracks, low-energy S fluorescence x-rays are attenuated by a few micrometers of a high-density mineral (e.g., Fe-sulfide) or compacted aerogel. Because most keystones are ~300 μm thick, a first-order correction, which assumed that all the S is shielded by ~150 μm of 20 mg/cm^3 of aerogel (*1*), would increase the abundance of S by no more than a factor of two, which does not provide consistency with CI at the 2σ level. However, some S is finely distributed in compacted or melted aerogel (*7*), possibly large enough to attenuate S fluorescence, and micrometer-size sulfide grains attenuate the S fluorescence, so the full effect of attenuation cannot be assessed without a detailed knowledge of the shape or size of aerogel and sulfide grains along each track. Selenium abundance is well correlated with S in meteoritic minerals. Although we detected Se in only 9 tracks, the mean Se abundance is nearly CI. If S and Se are correlated in the Wild 2 particles and have similar behavior during capture, then S in the whole-track data may be underestimated.

The size at which the composition of an aggregate converges to the average composition is an indication of the grain size of the material. Fine-grained, chondritic interplanetary dust particles (IDPs) of ~10 μm size (*12*), aggregates typically containing >10^4 grains, generally show only a factor-of-two variation in major elements and less than a factor-of-five variation in minor elements (*13*). Primitive chondritic meteorites, which contain much larger grains, show much greater variation in composition in samples up to millimeters in size. Because the largest track and the largest crater each have a composition significantly different from the mean (Fig. 2), Wild 2 dust is heterogeneous at the largest size scale of particle that we analyzed, showing greater compositional diversity than ~10 μm IDPs.

Before the Stardust mission, the only direct measurement of the elemental composition of comet dust came from impact-ionization mass spectrometers on the Giotto and VEGA spacecraft (*14*) that analyzed dust from comet 1P/Halley in 1986. The impact-ionization yields are uncertain, but the mean abundances of major refractory elements in Halley dust are reported to be within a factor of two of CI (*15*), although Fe, Cr, Mn, and Ni were depleted relative to Mg. These Halley results were based on the analysis of <1 ng of comet material.

The Wild 2 particles in the 23 keystones contain ~21 ng of Fe. Assuming the CI Fe content, the total mass of Wild 2 material in these tracks is ~115 ng. The crater residue resulted from the impact of ~215 ng of material (table S2). Taken together, we analyzed material from >300 ng of Wild 2 dust, several orders of magnitude more material than was analyzed at comet Halley. Even so, only 10% of the Stardust aerogel cells and a comparable fraction of the Stardust Al foils have been examined thus far. Comprehensive elemental analysis of the remaining material should provide a better mean S content and decrease the uncertainty in other element abundances.

The composition data on Wild 2 particles are generally consistent with but greatly extend the measurements at comet Halley because of the larger sample mass that we analyzed, coupled with the ability to analyze this material with the use of high-sensitivity instruments in state-of-the-art laboratories on Earth. The Wild 2 material appears depleted in S and Fe relative to Si and enriched in the moderately volatile minor elements Cu, Zn, and Ga as compared to CI. Both of these effects were previously reported in the fine-grained, anhydrous IDPs (*16*, *17*), some of which have inferred atmospheric entry speeds that suggest a cometary origin (*18*). The CI meteorite element abundances are presumed to represent the solar nebula composition for nonvolatile elements because of the good agreement between CI abundances and the composition of the solar photosphere (*6*). However, the abundances of Cu, Zn, and Ga are not well determined in the solar photosphere (*6*), which suggests that the Wild 2 particles and the anhydrous IDPs may better reflect the composition of the solar nebula for these moderately volatile elements.

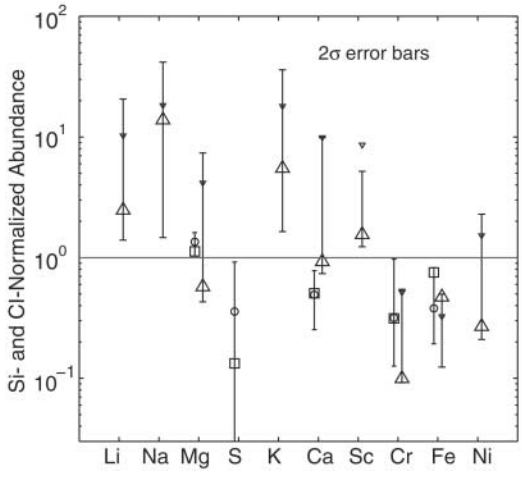

Fig. 4. CI- and Si-normalized average composition determined by summing the seven crater residue analyses (squares at Mg, S, Ca, Cr, and Fe) and by summing the same data set except for the largest crater (circles). The largest crater was produced by a particle having 82% of the total mass contributed by all seven particles, but the trend in the data is the same in both data sets, indicating that the mean composition is not significantly perturbed by the largest particle. TOF-SIMS results for five craters are also shown (large triangles at Li, Na, Mg, K, Ca, Sc, Cr, Fe, and Ni give the five-crater mean whereas the smaller triangles give the mean excluding the largest crater). The vertical bars show the 2σ statistical uncertainty (*4*).

References and Notes

1. P. Tsou *et al.*, *J. Geophys. Res.* **109**, E12S01 (2004).
2. A. J. Westphal *et al.*, *Meteorit. Planet. Sci.* **39**, 1375 (2004).
3. G. J. Flynn, F. Hörz, S. Bajt, S. R. Sutton, *Lunar Planet. Sci.* **XXVII**, 369 (1996).
4. See the supporting material on *Science* Online.
5. K. Lodders, *Astrophys. J.* **591**, 1220 (2003).
6. E. Anders, N. Grevese, *Geochim. Cosmochim. Acta* **53**, 197 (1989).
7. M. E. Zolensky *et al.*, *Science* **314**, 1735 (2006).
8. S. A. Sandford *et al.*, *Science* **314**, 1720 (2006).
9. A. T. Kearsley *et al.*, *Meteorit. Planet. Sci.*, in press.
10. A. T. Kearsley, M. J. Burchell, F. Hörz, M. J. Cole, C. S. Schwandt, *Meteorit. Planet. Sci.* **41**, 167 (2006).
11. F. Hörz *et al.*, *Science* **314**, 1716 (2006).
12. D. E. Brownlee, in *Properties and Interactions of Interplanetary Dust*, Proceedings of the Eighty-fifth Colloquium, Marseille, France, 9–12 July 1984 (Reidel, Dordrecht, Netherlands, 1985), pp. 143–147.
13. G. J. Flynn, S. R. Sutton, in *Proceedings of the 20th Lunar and Planetary Science Conference* (Lunar and Planetary Institute, Houston, TX, 1990), pp. 335–342.
14. J. Kissel, in *Advances in Mass Spectroscopy 1985, Proceedings of the 10th International Mass Spectrometry Conference*, Swansea, UK, 9–13 September 1985 (Wiley and Sons, Hoboken, NJ, 1986), pp. 175–184.
15. E. K. Jessberger, *Space Sci. Rev.* **90**, 91 (1999).
16. L. S. Schramm, D. E. Brownlee, M. M. Wheelock, *Meteoritics* **24**, 99 (1989).
17. G. J. Flynn *et al.*, in *Physics, Chemistry, and Dynamics of Interplanetary Dust*, B. Å. S. Gustafson, M. S. Hanner, Eds. (Astronomical Society of the Pacific, San Francisco, 1996), pp. 291–294.
18. D. E. Brownlee *et al.*, *Lunar Planet. Sci.* **XXIV**, 205 (1993).

19. Four synchrotrons used in this effort are national user facilities supported in part by the U.S. Department of Energy, Office of Science, Office of Basic Energy Sciences, under contract numbers (with managing institutions in parentheses) DE-AC02-05CH11231 (Advanced Light Source, University of California), DE-AC02-06CH11357 (Advanced Photon Source, University of Chicago Argonne, LLC), DE-AC02-98CH10886 (National Synchrotron Light Source, Brookhaven Science Associates), and DE-AC03-765F00515 (Stanford Synchrotron Radiation Laboratory, Stanford University). Experiments were performed at the BL47XU in the SPring-8 with the approval of the Japan Synchrotron Radiation Research Institute. The European Synchrotron Radiation Facility provided synchrotron radiation facilities. Stardust was the fourth flight project of NASA's Discovery Program.

Supporting Online Material

www.sciencemag.org/cgi/content/full/314/5806/1731/DC1
SOM Text
Figs. S1 to S11
Tables S1 to S4
References

10 October 2006; accepted 20 November 2006
10.1126/science.1136141

REPORT

Mineralogy and Petrology of Comet 81P/Wild 2 Nucleus Samples

Michael E. Zolensky,[1]* Thomas J. Zega,[2] Hajime Yano,[3] Sue Wirick,[4] Andrew J. Westphal,[5] Mike K. Weisberg,[6] Iris Weber,[7] Jack L. Warren,[8] Michael A. Velbel,[9] Akira Tsuchiyama,[10] Peter Tsou,[11] Alice Toppani,[12,13] Naotaka Tomioka,[14] Kazushige Tomeoka,[14] Nick Teslich,[12] Mitra Taheri,[2] Jean Susini,[15] Rhonda Stroud,[2] Thomas Stephan,[7] Frank J. Stadermann,[16] Christopher J. Snead,[5] Steven B. Simon,[17] Alexandre Simionovici,[18] Thomas H. See,[19] François Robert,[20] Frans J. M. Rietmeijer,[21] William Rao,[22] Murielle C. Perronnet,[1] Dimitri A. Papanastassiou,[23] Kyoko Okudaira,[3] Kazumasa Ohsumi,[24] Ichiro Ohnishi,[14] Keiko Nakamura-Messenger,[8] Tomoki Nakamura,[25] Smail Mostefaoui,[20] Takashi Mikouchi,[26] Anders Meibom,[20] Graciela Matrajt,[27] Matthew A. Marcus,[28] Hugues Leroux,[29] Laurence Lemelle,[18] Loan Le,[8] Antonio Lanzirotti,[30] Falko Langenhorst,[31] Alexander N. Krot,[32] Lindsay P. Keller,[1] Anton T. Kearsley,[33] David Joswiak,[27] Damien Jacob,[29] Hope Ishii,[12] Ralph Harvey,[34] Kenji Hagiya,[35] Lawrence Grossman,[17,36] Jeffrey N. Grossman,[37] Giles A. Graham,[12] Matthieu Gounelle,[20,33] Philippe Gillet,[18] Matthew J. Genge,[38] George Flynn,[39] Tristan Ferroir,[18] Stewart Fallon,[12] Denton S. Ebel,[40] Zu Rong Dai,[12] Patrick Cordier,[29] Benton Clark,[41] Miaofang Chi,[12] Anna L. Butterworth,[5] Donald E. Brownlee,[27] John C. Bridges,[42] Sean Brennan,[43] Adrian Brearley,[21] John P. Bradley,[12] Pierre Bleuet,[15] Phil A. Bland,[33,38] Ron Bastien[8]

The bulk of the comet 81P/Wild 2 (hereafter Wild 2) samples returned to Earth by the Stardust spacecraft appear to be weakly constructed mixtures of nanometer-scale grains, with occasional much larger (over 1 micrometer) ferromagnesian silicates, Fe-Ni sulfides, Fe-Ni metal, and accessory phases. The very wide range of olivine and low-Ca pyroxene compositions in comet Wild 2 requires a wide range of formation conditions, probably reflecting very different formation locations in the protoplanetary disk. The restricted compositional ranges of Fe-Ni sulfides, the wide range for silicates, and the absence of hydrous phases indicate that comet Wild 2 experienced little or no aqueous alteration. Less abundant Wild 2 materials include a refractory particle, whose presence appears to require radial transport in the early protoplanetary disk.

The nature of cometary solids is of fundamental importance to our understanding of the early solar nebula and protoplanetary history. Until now, we have had to study comets from afar using spectroscopy or settle for analyses of interplanetary dust particles (IDPs) of uncertain provenance. We report here mineralogical and petrographic analyses of particles derived directly from comet 81P/Wild 2.

All of the Wild 2 particles we have thus far examined have been modified in various ways by the capture process, in which cometary particles punched into the silica aerogel capture media, making various types of tracks and disaggregating into grains distributed along the tracks. All particles that may have been loose aggregates ("traveling sand piles") disaggregated into individual components, with the larger, denser components penetrating more deeply into the aerogel, making thin tracks with terminal grains (fig. S1). Individual grains experienced heating effects that produced results ranging from excellent grain preservation to melting (Fig. 1); such behavior was expected (*1*–*3*). What is remarkable is the extreme variability of these modifications and the fact that unmodified and severely modified materials can be found within 1 μm of each other, requiring tremendous local temperature gradients. Fortunately, we have an internal gauge of impact collection heating. Fe-Ni sulfides are ubiquitous in the Wild 2 samples and are very sensitive indicators of heating, and accurate chemical analyses can reveal which have lost S and which have not (and are therefore stoichiometric) (Fig. 2). Our surveys show that crystalline grains are found along the entire lengths of tracks, not just at track termini (fig. S1).

There appears to be very limited contamination from the spacecraft in the aerogel. Potential problems with secondary impacts (cometary grains striking the spacecraft, ricocheting, and splashing onto the aerogel) failed to materialize (*4*).

We have harvested samples from 52 tracks and have obtained a substantial understanding of the mineralogy of 26 of these. These tracks were chosen at random from those of average length. Analyses have also been performed on impact residues in seven aluminum foil craters >50 μm in diameter and on over 200 craters <5 μm in diameter (*5*). Crystalline materials are abundant in comet Wild 2 and many are coarse-grained relative to the submicrometer scales characteristic of many anhydrous IDPs and interstellar dust populations (*6*). Of the best-studied 26 tracks, 8 are dominated by olivine [$(Mg,Fe)_2SiO_4$] grains (tracks 1, 22, 26, 43, 57, 68, 71, and 77); 7 by low-Ca pyroxene [$(Mg,Fe)SiO_3$] (tracks 17, 20, 24, 27, 32, 41, and 69); 3 by a fairly equal amount of olivine and pyroxene (tracks 5, 10, and 35); and the remaining 8 by other minerals, mainly Fe-Ni sulfides. One of the latter tracks contains predominantly refractory minerals, one contains Na-silicate minerals, and five (tracks 36, 38, 42, 52, and 59) are dominated by ~5-μm-sized sulfide grains. These results suggest that crystalline materials are abundant in Wild 2.

In the seven large craters in aluminum foil that we examined, one contains only remnants of stoichiometric olivine, three are dominated by Mg-